scientific reports

Check for updates

OPEN

# Antibacterial activity of the novel peptide Pac-525 with the RGD motif against intracellular *Escherichia coli*

Martina Coufalova[1], Miguel A. M. Rodrigo[1], Hana Michalkova[1], Vedran Milosavljevic[1], Kristýna Hrazdilova[1,2], Ludek Zurek[1,3] & Kristyna Cihalova[1,3]✉

**Infections caused by invasive intracellular bacteria pose major therapeutic challenges due to pathogen survival and growth inside of host cells as well as the low intracellular accessibility for conventional antibiotics. The limited ability of most antibiotics to enter intracellular compartments underscores the urgent need for innovative antimicrobial agents capable of overcoming these barriers. In this study, the antibacterial peptide Pac525 was synthesized with the RGD domain to facilitate efficient penetration into eukaryotic cells. The efficacy and safety of RGD-Pac525 was evaluated in intracellular infection models, using the macrophage cell line RAW 264.7, chicken intestinal organoids, and chicken embryo tissues via the chorioallantoic membrane (CAM). Our findings from cell line experiments demonstrate that the RGD-Pac525 peptide retained the antimicrobial properties of the original peptide without compromising its efficacy. While RGD-Pac525 reduced the intracellular adherent-invasive pathogen *Escherichia coli* KV203 by 50% in RAW 264.7 macrophage cells, it did not adversely affect the macrophage viability. Additionally, RGD-Pac525 effectively reduced the intracellular bacterial burden in organoids, without compromising their structural integrity. In ovo bioassays, a substantial reduction in the bacterial load was observed in liver and intestinal tissues, indicating the peptide ability to achieve systemic distribution and to overcome tissue barriers. RGD-Pac525 was effective in infection models by suppressing bacterial growth. Preliminary observations suggest it may also affect host responses, indicating a potential for combined antimicrobial and therapeutic effects that warrant further studies. This study provides a compelling proof of concept for utilizing RGD-modified antimicrobial peptides for treatment of intracellular bacterial infections.**

**Keywords** Intracellular infections, Antibacterial peptide, RGD-Pac525, Organoid, CAM assay

Intracellular (IC) bacterial infections pose serious health and economic threats due to bacterial ability to evade humoral immune responses and antimicrobial treatments[1]. The intracellular environment provides protection from extracellular factors and contributes to the chronic and recurrent nature of IC infections[2]. Intracellular *E. coli* include uropathogenic (UPEC), enteroinvasive (EIEC), and adherent-invasive (AIEC) pathotypes that employ various strategies to survive within host cells[3,4]. These include evading exocytic processes, escaping into the host cell cytoplasm, spreading laterally among cells, and re-entering through the basolateral plasma membrane[5]. AIECs can migrate deep to tissues, continuously activate macrophages, and potentially induce granuloma formation, characteristic of Crohn's disease lesions[6–8]. The destabilization of the intestinal barrier occurs directly via invasive properties of bacteria or indirectly through macrophage activation leading to production of pro-inflammatory cytokines and persistent intestinal inflammation[9].

The treatment of IC infections is challenging due to the limited permeability of conventional antibiotics into eukaryotic cells[10,11] and their low antimicrobial activity in the acidic intracellular environment[12–16]. In addition, inadequate efficacy of antibiotics against IC pathogens may promote selection of resistant mutants[17]. These challenges highlight the need for novel approaches in the treatment of intracellular infections.

[1]Department of Chemistry and Biochemistry, Mendel University in Brno, Zemedelska 1, 613 00 Brno, Czech Republic. [2]Faculty of Medicine in Pilsen, Biomedical Center, Charles University, Pilsen, Czech Republic. [3]Department of Microbiology, Nutrition and Dietetics, Czech University of Life Sciences, Prague, Czech Republic. ✉email: kriki.cihalova@seznam.cz

The promising alternatives to conventional antibiotics are antimicrobial peptides (AMPs). These peptides are natural components of the innate immune system with a broad-spectrum antibacterial, antiviral, anti-parasitic, and antitumor activity[18–21] and potential to modulate the host immune responses[22]. It has been shown that the antibacterial effects of AMPs involve disrupting bacterial cell membranes and interfering with bacterial intracellular processes[21,23,24]. Antimicrobial peptides preferentially target the negatively charged surface of bacterial cells[25] which limits their penetration into eukaryotic cells and poses a challenge for treatment of intracellular infections. Therefore, it is necessary to devise a strategy for intracellularization of the drug. One of those strategies is the combination of AMPs with the arginine-glycine-aspartic acid (RGD) motif that is recognized by integrin glycoproteins on the eukaryotic cell surface followed by internalization[26,27].

In order to overcome limitations of AMPs derived from natural sources, such as low stability, poor salt tolerance, and high toxicity[28]synthetic peptides with enhanced properties have been developed[18]. The synthetic peptide Pac-525 has demonstrated efficacy against several microbial taxa, including *E. coli*, *Pseudomonas aeruginosa*, *Staphylococcus aureus* (including methicillin-resistant strains), *S. epidermidis*, *Candida albicans*, and *Fusarium solani*[29–32].

To evaluate the potential of synthetic peptides for treatment of intracellular bacterial infections, in ovo models provide a unique platform to study the antibacterial efficacy of peptides in a complex, yet controlled biological system, mimicking the multicellular environment[33,34]. Similarly, intestinal organoids derived from primary tissues offer a physiologically relevant three-dimensional system to assess peptide antibacterial activity and interactions with the host cells[35,36]. These approaches not only enhance our understanding of peptide efficacy but also bridge the gap between simplified in vitro models and in vivo systems and provide valuable insights into peptide functionality in a host-like environment.

This study focused on the efficacy of the synthesized peptide Pac-525 combined with RGD tripeptide against intracellular AIEC *E. coli* KV203 in the macrophage cell line, the chicken intestinal organoid model, and the chorioallantoic membrane (CAM) assay[37,38]. By employing these approaches, this study seeks to explore the potential of the RGD-Pac525 peptide as a therapeutic agent for treatment of intracellular bacterial infections.

## Materials and methods

### Chemicals

All chemicals and reagents were purchased from Sigma-Aldrich (St. Louis, MO, USA) with purity meeting the standards of the American Chemical Society (ACS), unless noted otherwise.

### Peptides, cell lines, and bacterial cultures

Peptides RGD (H-RGD-OH), Pac525 (H-KWRRWVRWI-OH), and RGD-Pac525 (HRGDKWRRWVRWI-OH) were purchased, all with purity > 96%, from HENA s.r.o., Banov, Czech Republic (Supplementary Table S1). Synthesized and freeze-dried peptides were stored at – 20 °C. The macrophage RAW 264.7 cell line was purchased from American Type Culture Collection (Manassas, VA, USA); cells were maintained in Dulbecco's Modified Eagle's Medium (DMEM) supplemented with 10% Fetal Bovine Serum (FBS), 100 U/ml penicillin and 0.1 mg/ml streptomycin in a humidified atmosphere containing 5% $CO_2$ at 37 °C. The murine macrophage cell line RAW 264.7 was selected for its widespread use and well-established role as a model for investigating bacterial uptake, survival, and intracellular trafficking in phagocytic immune cells[39]. Its application is particularly prominent in studies of bacterial virulence, including that of *E. coli*, due to its functional parallels with innate immune cells that mediate early host-pathogen interactions. *Escherichia coli* KV203 was obtained from the Faculty of Medicine, Masaryk University, Brno, Czech Republic[40] (Supplementary Table S2). Bacteria were cultured on Mueller Hinton (MH) agar and incubated at 37 °C for 24 h or in Miller Luria Bertani (LB) broth at 37 °C for 24 h, depending on the experiment.

### Cell viability: MTT assay

The short-term effect of peptides on cell viability was assessed using the MTT (3(4,5dimethylthiazol-2-yl)-2,5-diphenyltetrazolium bromide) assay. The macrophage cell suspension (5000 cells/50 µl of media per well) was incubated for 24 h at 37 °C with 5% $CO_2$. RAW 264.7 cells at passage 6 were used for all experiments. Peptides were dissolved in ACS-grade water prior to dilution in the culture medium. At 60–80% confluence, the peptide at concentration of 500 to 1.95 µg/ml was added. After 24 h, 10 µl of 5 mg/ml MTT dye solution was added. After 3 h of incubation, the medium containing MTT solution was replaced with 100 µl of 99.9% dimethyl sulfoxide (DMSO), incubated for 5 min and the absorbance of the samples was determined using Infinite 200 PRO (λ = 570 nm) (Tecan, Männedorf, Switzerland). Control cells treated only with the culture medium were considered 100% viable, and the reduction in cell viability by more than 30% ($IC_{70}$) was considered cytotoxic according to the ISO 10993-5 guidelines[41].

### Bacterial growth and viability

The antibacterial activity of peptides against *E. coli* KV203 was determined via absorbance measurements using the Bioscreen C MBR system (Oy Growth Curves Ab Ltd., Finland) at an optical density of 600 nm ($OD_{600nm}$). Using a 100-well honeycomb plate, the studied peptides were serially diluted two-fold in Phosphate-Buffered Saline (PBS) at concentrations from 1000 µg/ml to 1.95 µg/ml and *E. coli* KV203 in double-concentrated Mueller-Hinton broth was added to each well, resulting in final peptide concentrations ranging from 500 µg/ml to 0.98 µg/ml and the final inoculum concentration of $4.0 \times 10^5$ CFU/ml. Bacteria were incubated in the Bioscreen C MBR at 37 °C for 24 h, and the growth (absorbance) was measured every 30 min. The control treatment was set up as above with PBS instead of peptides. All experiments were conducted in three independent biological replicates, each performed in a technical triplicate ($n = 9$).

Based on growth curves, minimal inhibition concentration (MIC) and $MIC_{50}$ were calculated. The relative optical density (%) was determined from the absorbance value after 24 h and compared to the absorbance value of control (considered 100%).

## Cell infection and treatment

For cell infection and treatment, a modified gentamicin-protection assay was used[42] with following specifications. RAW 264.7 cells were seeded at a density of $1.5 \times 10^5$ cells per well in 24-well plates, and allowed to adhere overnight in a humidified atmosphere containing 5% $CO_2$ at 37 °C. The cell medium was removed, and cells were infected with *E. coli* KV203 (multiplicity of infection, MOI, 100:1) by incubating the cultures with DMEM containing the bacteria supplemented with 10% FBS without antibiotics (0.5 ml). After a two-hour infection period, cell monolayers were washed with PBS and treated with the cell medium containing gentamicin (100 µg/ml) for one hour to kill extracellular bacteria.

For the infection treatment, the medium was replaced with the fresh cell medium containing the peptide (250 µg/ml) and gentamicin (100 µg/ml), to prevent the extracellular growth of *E. coli*) and incubated for 4 h. After that, the medium was removed, cell monolayers were washed with PBS and lysed with Triton X-100 (1.0% w/v) for 10 min. The obtained cell lysates were serially diluted in PBS and seeded on Mueller-Hinton agar plates, which were incubated for 16–20 h at 37 °C and then the number of CFUs were counted. This assay was carried out as two independent experiments (biological replicates), each in technological pentaplicate for every peptide and control ($n = 10$). One-way ANOVA and Dunnett's Test were used for the statistical analysis.

## Peptide fluorescent labelling

To visually confirm the penetration of the conjugated peptide across the cell membrane of eukaryotic cells, the synthesized peptides were labelled with the fluorescent dye Rhodamine B (acryloxyethyl thiocarbamoyl rhodamine B). The peptide, at a concentration of 1.0 mg/ml, was incubated overnight with Rhodamine B at a final concentration of 100 µg/ml at room temperature under continuous rotation. Unbound dye was removed using the Pur-A-Lyzer Midi Dialysis Kit (Sigma-Aldrich, USA), and the result was confirmed by gel electrophoresis (data not shown).

## *Escherichia coli* KV203 transformation with pGLO-GFP plasmid

Competent cells were prepared according to the manufacturer's protocol[43]with minor modifications. An overnight culture of *E. coli* KV203 was diluted 1:100 into 50 ml of fresh LB broth. The centrifugation step was repeated five times with resuspension three times in 500 µl of ice-cold 10% glycerol, followed by 250 µl and 100 µl, to achieve a high concentration of competent cells. For electroporation 50 µl of competent cells with 1 µl of pGLO-GFP plasmid DNA of concentration 50 ng/µl were mixed and electroporated (2.5 kV, 200 Ω, and 25 µF). The transformed cells were incubated at 37 °C for 1 h with shaking at 250 rpm and 100 µl of the transformation mixture was plated onto LB agar containing 100 µg/ml ampicillin and inducers, such as arabinose, for GFP expression, and incubated overnight at 37 °C. The next day, plates were observed for colony growth and checked for GFP expression under UV light.

## Verification of peptide entrance to eukaryotic cells

To study the ability of peptides to penetrate into the RAW 264.7 cell line, approximately $10^5$ cells were seeded on the bottom of µDish 35 mm (ibidi GmbH, Gräfelfing, Germany) and left to adhere overnight. The DMEM medium was replaced with the fresh medium containing Rhodamine B-labelled peptides (RGD, Pac525 or RGD-Pac525) at the concentration of 250 µg/ml for 4 h, after which the cells were washed with prewarmed (37 °C) PBS. Visualization was carried out using the Axio Imager D1 confocal microscope (Carl Zeiss, Germany).

## Imaging of infected cells

RAW 264.7 cells were seeded in µ-Dish and left to adhere overnight. The medium was removed, and DMEM containing pGLO-GFP-transformed *E. coli* KV203, supplemented with 10% FBS and no antibiotics, was added to the cells. Cells were then incubated for 2 h at 37 °C in a humidified atmosphere. The infection was carried out at an MOI 100:1. Subsequently, cell monolayers were washed with prewarmed PBS and treated with the cell medium supplemented with gentamicin (100 µg/ml) for one hour to kill extracellular bacteria, after which cells were washed with prewarmed PBS. Visualization was carried out using the Axio Imager D1 confocal microscope (Carl Zeiss, Germany).

## Generation of 3D chicken intestinal organoids

The fertilized chicken eggs purchased from a local provider (INTEGRA, a. s., Zabcice, Czech Republic) were incubated with rotation at 37.5 °C and 65% humidity for 15 days. The full intestine was removed, cut open longitudinally into 3 mm sections and collected in ice-cold PBS. The intestinal crypts were isolated from the tissue using a previously established protocol[44] with slight modifications. In brief, the intestine sections were washed with ice-cold PBS until most luminal contents were cleared, and the villi were scraped off with a coverslip. After an additional washing with ice-cold PBS, the intestine was transferred to a 50 ml tube. Twenty ml of ice-cold PBS were added, and the fragments were washed by gently pipetting them up and down with a 10 ml pipette. The supernatant was discarded after settling. This washing step was repeated 10 times until the supernatant was almost clear. Then, 20 ml of ice-cold crypt isolation buffer (5 mM EDTA in PBS) were added, and the tube was gently rocked at 4 °C for 30 min. The tissue in solution was pipetted up and down every 10 min. After the fragments settled, the supernatant was removed, and 20 ml of ice-cold PBS was added to wash the fragments using a pipette. This procedure was repeated until most crypts had settled, and the crypt fractions were passed through a pluriStrainer Mini 70 µm system (pluriSelect, Leipzig, Germany). The intestinal crypts

were collected into 50 ml tube(s) after adding 5% FBS to the crypt solution. The crypt fractions were centrifuged at 300 × g for 5 min and resuspended in 20 ml of organoid culture medium (advanced Dulbecco's modified Eagle medium/F12 supplemented with penicillin/streptomycin, 10 mmol/l HEPES, Glutamax), quantification of live/dead cells by the Countess FL II Automated Cell Counter (Thermo Fisher Scientific, Waltham, MA, USA), and seeded onto mini petri plates and incubated at 37 °C, 5% $CO_2$.

### *Escherichia coli* KV203 colonization of chicken intestinal organoids

Six-day-old organoids in a mini petri plate (each plate containing several organoids cultured in the defined volume of the medium) were colonized with *E. coli* KV203 pGLO-GFP (100,000 CFU in 20 µl) for 5 min. Subsequently, RGD-Pac525 (50 µg in 100 µl) was added to the organoid medium and PBS was used in the control group. After 2 h of incubation at 37 °C with 5% $CO_2$, organoids were examined using the EVOS FL Auto Cell Imaging System (Thermo Fisher Scientific). The green fluorescence emitted by *E. coli* KV203 was captured at 488 nm using the GFP light cube (Thermo Fisher Scientific). To observe whether the bacterial invasion occurred inside the organoids after 2 h post-infection, the organoids were centrifuged, the medium was replaced with fresh medium, and organoids were microscopically examined.

### The in Ovo chicken embryo Chorioallantoic membrane (CAM) assay

Fertilized chicken eggs were obtained from the Integra Farm (INTEGRA, a. s., Zabcice, Czech Republic) were incubated with rotation at 37.5 °C and 65% humidity for 10 days. To create an opening in the egg and to prepare the CAM for pre-infection steps, a protocol described previously was followed[45]. The CAMs were then infected with a 25 µl dose of *E. coli* KV203 pGLO-GFP inoculum (40.000 CFU/ml) applied topically. After 15 min. of incubation, RGD-Pac525 (25 µg in 50 µl) was directly administered onto each CAM. The embryos were left undisturbed for 30 min to allow for the absorption of RGD-Pac525 at the infection site and to prevent embryonic death. Control CAMs were treated with 50 µl of RGD-Pac525 without bacteria. Eggs were then incubated for additional 48 h.

To fluorescently label the blood circulation, 50 µl of 10 µg/ml of LCA solution (Vector laboratories, Burlingame, CA, USA) was injected at indicated time-points to the peripheral veins of the viable CAM using a 30G hypodermic needle. Then, portions of the CAM, brain, liver and intestine were harvested to perform additional analyses, and to localize *E. coli* KV203 in the tissues. The EVOS FL Auto Cell Imaging System (Thermo Fisher Scientific, Waltham, MA, USA) was used to detect the emitted green light from *E. coli* KV203, and red light from the rhodamine labelled peptide. To quantify vascular density on the CAM, the tissue was harvested at the end of the experiment and micrographs were captured from the bottom side using a stereomicroscope (DSTM 723 W 1.3 with digital video-camera). The micrographs were then analyzed for vascular density using the Vessel Analysis tool in ImageJ software (NIH). To locate the infection of *E. coli* KV203 in chicken brain, liver and intestine, the tissues were manually homogenized, serially diluted in PBS and inoculated on petri dishes with MH agar. After over-night cultivation at 37 °C, the CFUs were counted.

## Results

### Peptide antimicrobial activity

The antimicrobial activity of Pac525 and its conjugate with the RGD domain was assessed by monitoring the growth curves using planktonic *E. coli* KV203 and determination of the minimum inhibitory concentration (MIC) (Fig. 1a). The resulting MIC values for Pac525 and the RGD-Pac525 conjugate were 62.5 µg/ml and 125.0 µg/ml, respectively. The optical density of *E. coli* KV203 was calculated relative to the control group that did not receive any peptide treatment (Fig. 1b). The $MIC_{50}$ values were 41.0 µg/ml and 92.6 µg/ml for Pac525 and RGD-Pac525, respectively. The elevated values observed at higher concentrations of Pac525 and RGD-Pac525 were likely due to the optical properties of proteins at high concentrations, rather than actual bacterial growth, as no visible growth is observed in the corresponding growth curves (Fig. 1a). The RGD motif itself had no antimicrobial effect. These results show that the antimicrobial activity of peptide Pac525 is maintained upon synthesis with the RGD domain.

### Cell compatibility with the peptides

The cytotoxic effect of the peptides on the macrophage RAW 264.7 cell line was assessed using the standard MTT assay (Fig. 1c). The $IC_{70}$, as defined by the ISO 10933-5 guidelines[41] was 363.5 µg/ml for RGD, 330.88 µg/ml for Pac525 and 446.94 µg/ml for RGD-Pac525. At the highest concentration tested (500 µg/ml), the viability of cells was 52% for RGD, 40% for Pac525, and 61% for RGD-Pac525. Overall, the combination of antimicrobial peptide Pac525 with the RGD motif (RGD-Pac525) showed a lower cytotoxic effect compared to that of Pac525 alone.

### Visualization of intracellular bacteria

The ability of pGLO-GFP-*E. coli* KV203 to invade eukaryotic cells was confirmed and visualized by fluorescent microscopy. Green fluorescent bacteria were visible in the cytoplasm of RAW 264.7 macrophage cells after 2 h of infection (Fig. 2a).

### Verification of the drug entrance to RAW 264.7

The ability of the peptides to enter the intracellular space of RAW 264.7 macrophages was assessed by fluorescent microscopy. Our results showed that Rhodamine B-labelled RGD tripeptide attached exclusively to the surface of macrophage cells (Fig. 2bA). The red fluorescence was apparent on the entire cell surface. The binding or uptake of the Pac525 peptide was very limited, as only a few fluorescent cells were visible within the entire field (Fig. 2bC). In contrast, the labelled RGD-Pac525 peptide penetrated the cells, and the red fluorescence was

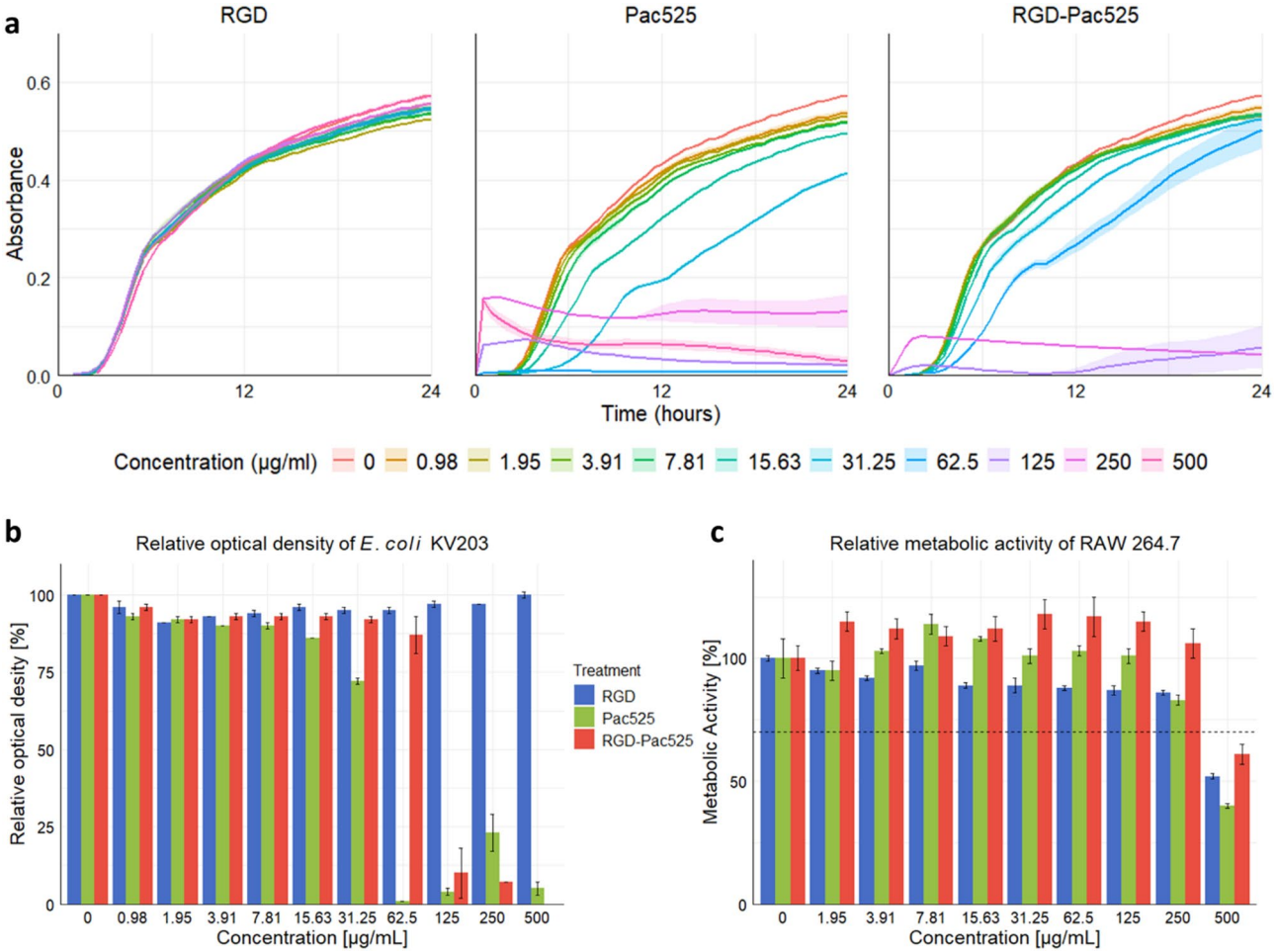


**Fig. 1**. Effects of antibacterial peptides on *E. coli* KV203 and RAW 264.7. (**a**) Bacterial growth curves at different concentrations of peptides RGD, Pac525, and RGD-Pac525. The results are expressed as the mean ± SEM ($n = 9$). (**b**) Relative optical density upon exposure to different concentrations of RGD, Pac525, and RGD-Pac525 after 24 h of treatment. Results are expressed as the mean % of control cells treated with the medium only and considered 100% viable ± SEM ($n = 9$). (**c**) RAW 264.7 cell metabolic activity upon exposure to different concentrations of RGD, Pac525, and RGD-Pac525 for 48 h (measured by the MTT assay). The dotted line indicates the cytotoxicity limit established by the ISO 10993-5 guidelines[41]. The results are expressed as the mean % of control cells treated with the medium only and considered 100% viable ± SEM ($n = 4$).

observed in the vesicle-like structures, demonstrating an intracellular, cytoplasmic localization of the peptide (Fig. 2bE).

## Antibacterial activity of peptides against intracellular *E. coli* KV203

The effect of the peptides on intracellular bacteria was also monitored by fluorescent microscopy. Intracellular bacteria were not affected by RGD (Fig. 2bB) and Pac525 (Fig. 2bD). In contrast, in the presence of RGD-Pac525 the link between the amount of labelled peptide in cells and the number of bacteria in their intracellular compartment was apparent (Fig. 2bF). In this case, the ibidi plate was not washed to remove planktonic bacteria to detect the effect of the peptide more clearly.

The ability of peptides to eliminate intracellular *E. coli* KV203 in infected macrophages was quantified by measuring the reduction in colony-forming units (CFUs) in lysates. The RGD and Pac525 peptides reduced the intracellular *E. coli* burden by 18.4% (RGD) and 23.6% (Pac525) while the efficacy of RGD-Pac525 more than doubled and reduced the intracellular bacteria by 50% ($p \leq 0.001$) (Fig. 2C).

## Antibacterial effect of RGD-Pac525 on *E. coli* KV203 in chicken 3D intestinal organoids

Generation of organoids from chicken intestines was successful, illustrating the onset of a budding structure that consisted of the central lumen and several surrounding crypt-like domains (Fig. 3a). The organoid cultures exhibited morphological diversity due to their self-organizing nature and developmental heterogeneity (Fig. S2a). The invasivity of *E. coli* KV203 was evaluated by comparison to that of the non-invasive strain *E. coli* DH10B. Fluorescent microscopic imaging of chicken 3D intestinal organoids infected with *E. coli* DH10B

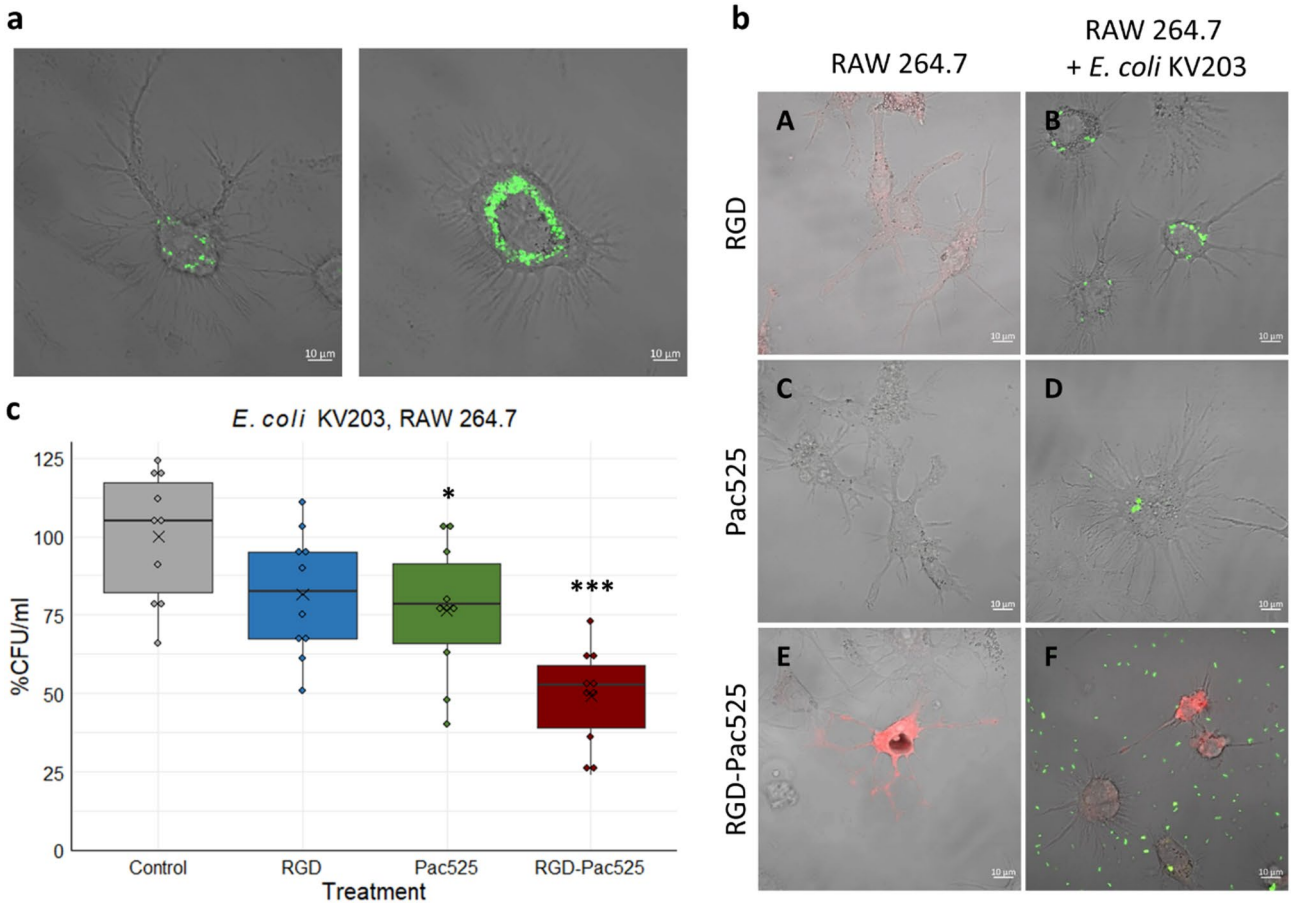


**Fig. 2**. Antibacterial activity of peptides against intracellular *E. coli* KV203. (**a**) RAW 264.7 macrophage cells successfully infected by pGLO-GPF *E. coli* KV203. (**b**) RAW 264.7 macrophage cells with green fluorescence of *E. coli* KV203 pGLO-GFP and red fluorescence from Rhodamine-B labelled peptides. (**bA**) RAW 264.7 cells treated with Rhodamine B-labelled RGD; (**bB**) RAW 264.7 cells infected with *E. coli* KV203 and treated with Rhodamine B-labelled RGD; (**bC**) RAW 264.7 cells treated with Rhodamine B-labelled Pac525; (**bD**) RAW 264.7 cells infected with *E. coli* KV203 and treated with Rhodamine B-labelled Pac525; (**bE**) RAW 264.7 cells treated with Rhodamine B-labelled RGD-Pac525; (**bF**) RAW 264.7 cells infected with *E. coli* KV203 and treated with Rhodamine B-labelled RGD-Pac525 without washing away planktonic extracellular bacteria. The unmerged individual channels are available in Fig. S1. (**c**) Intracellular antibacterial activity (expressed as the number of colony-forming units [CFUs]) of peptides in macrophage cell line RAW 264.7 infected with *E. coli* KV203 ($n = 10$). (*$p \leq 0.05$ and *** $p \leq 0.001$)

pGLO-GFP (Fig. S2b) revealed a minimal GFP signal, indicating that *E. coli* DH10B exhibited low invasivity and limited colonization of the organoids. In the identical experimental setup, fluorescence was observed within the organoid following the infection with *E. coli* KV203 (Fig. 3d) after extensive washing. This indicates that the fluorescent signal was not due to surface adherence or extracellular presence, but rather reflected the real bacterial invasion.

To examine the impact of RGD-Pac525 on invasion and growth of *E. coli* KV203 (pGLO-GFP), in vivo conditions were mimicked by exposing the bacteria to RGD-Pac525 two hours after infection. The treatment of infected organoids with RGD-Pac525 resulted in a significantly lower number of planktonic bacteria compared to that of untreated organoids (Fig. 3b). The reduction of bacteria in the medium after treatment was 85% compared to that of the untreated organoids (Fig. 3c). The effect of RGD-Pac525 on bacterial invasion to infected organoids 2 h post-infection was determined by detecting GFP-emission from *E. coli* after medium replacement. The GFP was detected in untreated organoids but not in the organoids treated with RGD-Pac525 (Fig. 3d).

## Effect of RGD-Pac525 on *E. coli* KV203 pGLO-GFP in Ovo

To assess the virulence of *E. coli* KV203 and the antibacterial effects of RGD-Pac525 using the CAM model, nine eggs were inoculated per each group. Infection of the CAM with *E. coli* KV203 pGLO-GFP resulted in 25% embryo mortality compared to no mortality in the group infected and subsequently treated with RGD-Pac525 at 48 h (Fig. 4a). Embryos infected with *E. coli* KV203 (with and without RGD-Pac525) showed a significantly lower weight compared to that of uninfected controls (Fig. 4b).

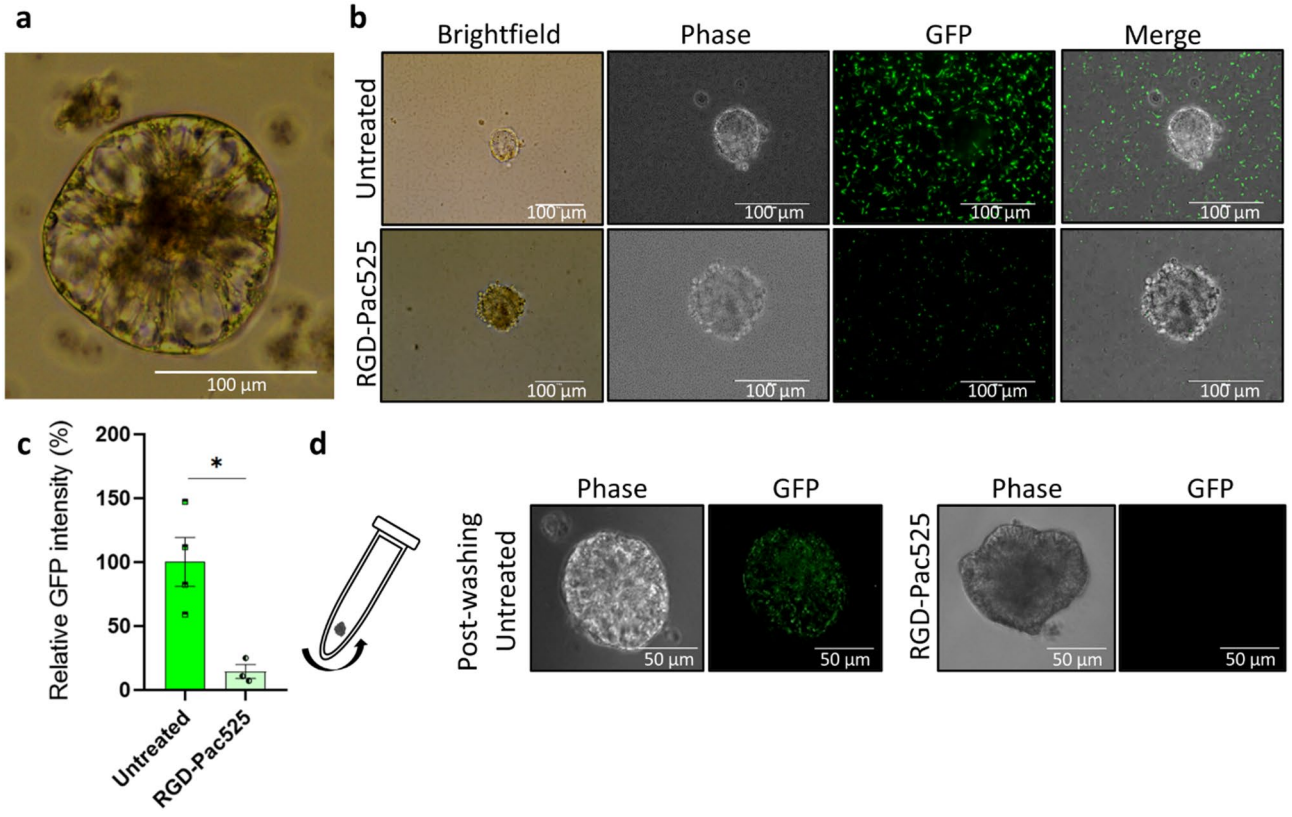


**Fig. 3**. Effect of RGD-Pac525 on chicken intestinal organoids infected by *E. coli* KV203. (**a**) The organoid morphology 6 days after the isolation of intestinal crypts from chicken tissue. (**b**) The impact of RGD-Pac525 (500 µg/ml) on *E. coli* KV203 (pGLO-GFP) growth inhibition in 6 days chick organoids after 2 h of treatment. (**c**) Relative GFP intensity (%) of *E. coli* KV203 with and without RGD-Pac525. Data represent mean ± SEM ($n \geq 3$). ($^*p < 0.05$). (**d**) Micrographs of *E. coli* KV203 in organoids 2 h post-infection with and without RGD-Pac525 (organoids were centrifuged, and the medium was replaced with fresh medium).

The effect of *E. coli* KV203 infection on CAM morphology and angiogenesis with and without RGD-Pac525 treatment for 48 h is shown in Fig. 4c. The quantification of vascular density (%) revealed higher vascularization and angiogenesis on the bottom side of the CAM in response to *E. coli* KV203 (± 20%) compared to that of the uninfected control (± 6.5%). A substantial inhibitory effect on the angiogenesis process was observed with a reduction of approximately 8% in the CAM after 48 h of RGD-Pac525 treatment (Fig. 4d).

Additionally, the in ovo CAM assay was performed to evaluate the inhibitory effects of RGD-Pac525 on the growth of *E. coli* KV203 in the CAM. *Escherichia coli* KV203 infection was successfully established on the upper CAM as indicated by the extensive GFP signal from the *E. coli* KV203 and the RGD-Pac525 visibly reduced the GFP signal of *E. coli* KV203 (Fig. 4e). The cross-sections of the infection sites in the CAM showed a thicker bacterial mass and a greater number of internal capillaries in the untreated group infected with *E. coli* KV203 compared to those treated with RGD-Pac525 (Supplementary Fig. S3).

Assessment of the invasion of *E. coli* KV203 from the CAM throughout the embryo and colonization of tissues showed that bacteria were able to colonize brain, liver, and intestinal tissue. In contrast, chickens treated with RGD-Pac525 showed a significant reduction ($^*p < 0.05$) of CFUs of *E. coli* KV203 in the liver and the intestine while significant differences were not observed in the brain tissue (Fig. 4f).

## Discussion

Conventional antibiotic treatments are largely ineffective against bacteria that can survive and proliferate in the intracellular environment of eukaryotic cells[17]. These treatments also face a growing challenge due to widespread loss of efficacy caused by acquired antibiotic resistance[20]. Therefore, it is crucial to explore new alternatives that target intracellular infections and that are less likely to develop resistance and that exhibit fewer side effects on the host.

In the present study, the antibacterial effect of the peptide Pac525 combined with the RGD domain for efficient penetration of eukaryotic cells was tested against the intracellular infection. Our results demonstrated that this peptide was able to successfully enter the intracellular space of eukaryotic cells and greatly lowered intracellular *E. coli* KV203 in the macrophage cell line, chicken intestinal organoids, and the chicken embryo tissues.

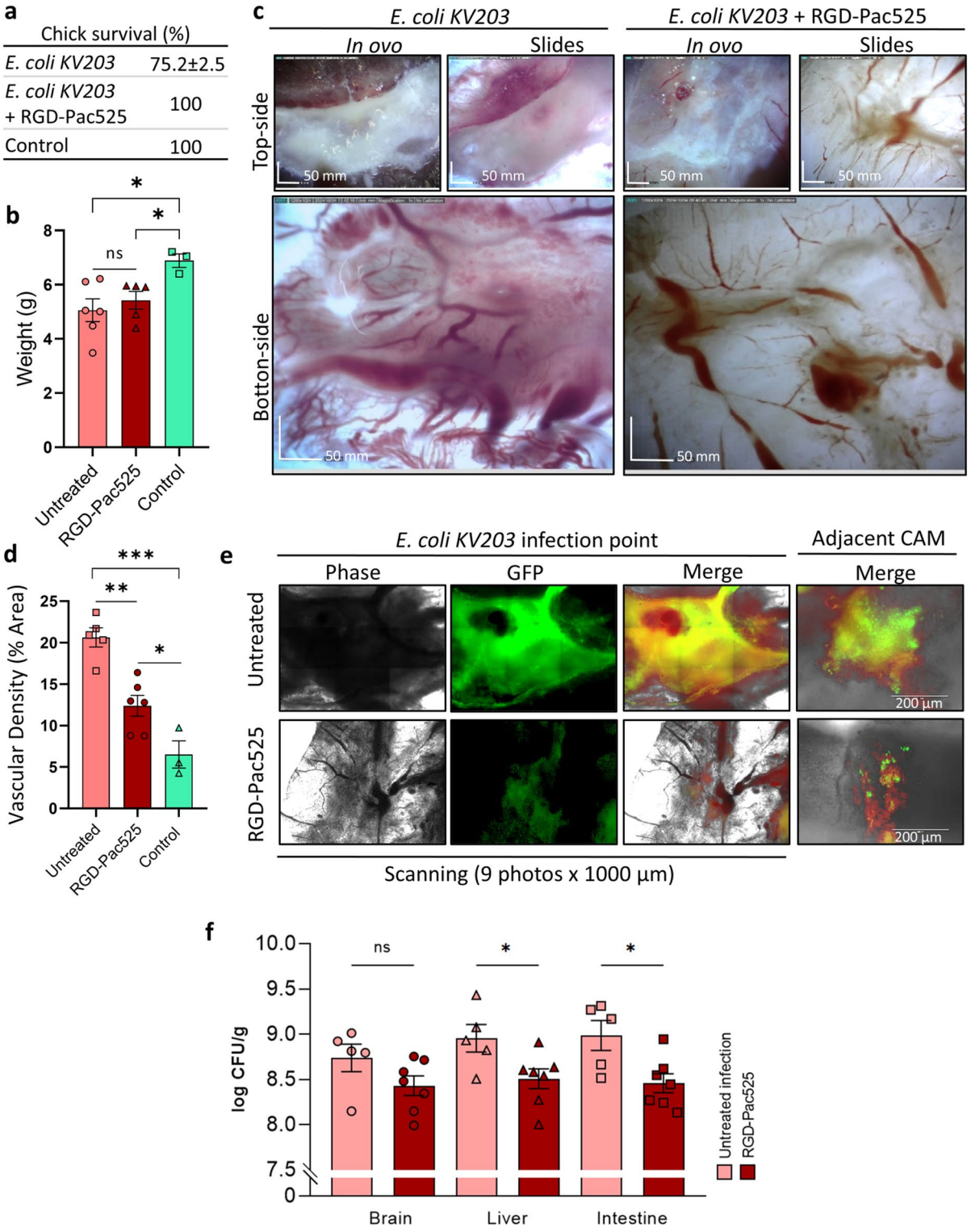


**Fig. 4**. Antibacterial effect of RGD-Pac525 on *E. coli* KV203 infections in ovo. (**a**) Embryo mortality (%) and (**b**) chick weight (g) after 48 h of *E. coli* KV203 infection ($n > 5$), compared to that of infected chickens treated with RGD-Pac525 ($n > 5$), and of uninfected chicks ($n = 3$). (**c**) Stereomicroscope images of the top and bottom sides of *E. coli* KV203 infection on the CAM treated with RGD-Pac525 for 48 h, compared to that of untreated control. Scale bar = 50 mm. (**d**) Quantification of vascular density (%) using the ImageJ Vessel tool. (**e**) Fluorescent imaging of *E. coli* KV203 infection in the CAM and distal CAM. Scale bar = 200 µm. (**f**) *E. coli* KV203 recovered from brain, liver, and intestine ($n > 5$) after 48 h of infection on the CAM. Data represent mean ± SEM. (*$p < 0.05$, **$p < 0.01$, ***$p < 0.001$)

The peptide Pac-525 was tested previously as a potent antimicrobial agent on modified surfaces for implanted biomaterials[46–51] where it was effective against *E. coli*, *S. aureus*, *Streptococcus sanguis*, *Fusobacterium nucleatum*, and *Porphyromonas gingivalis*. However, the combination of Pac-525 with the RGD domain and the testing against intracellular infections has not been explored previously.

The RGD-motif is a versatile ligand for active targeting of various cells and tissues[52]. For example, RGD-modified drug delivery systems have been exploited for active targeted delivery of therapeutic or diagnostic agents[53–62]. RGD peptides enable drug carriers to enter cells by interacting with integrin receptors on the cell surface. This receptor-dependent endocytosis enhances the intracellular uptake of drugs, thereby improving their therapeutic efficacy[63–66]. The role of the peptide size in determining the mechanism of cellular uptake via the RGD motif has been a subject of discussion[67]; however, regardless of the specific uptake mechanism, our study confirmed that combining the RGD domain with a short antimicrobial peptide enables its delivery to cell interior.

The combination of the RGD motif with Pac-525 preserved the peptide antimicrobial properties and did not compromise its efficacy. These findings indicate that the release of the Pac-525 from the RGD carrier is not required for its antimicrobial activity. This simplifies its application, as RGD-Pac525 does not depend on external stimuli such as pH, temperature or the presence of specific enzymes to trigger peptide release, unlike that of delivery systems used in previous studies[68–70].

To date, no clinical trials using antimicrobial peptides targeting intracellular bacteria have been successful. One of the reasons for the termination of clinical trials were the adverse effects of tested agents[71]. In our study, the MIC of RGD-Pac525 did not negatively affect the viability of the macrophage cell line RAW 264.7 suggesting no adverse effects on host cells. Furthermore, we employed additional approaches using in vivo bioassays including intestinal organoids and chicken embryos.

Organoids, as animal-free 3D culture systems composed of multiple cell types, represent a promising alternative to traditional animal models[72–74]. These systems provide a consistent and reproducible platform for simulating the microenvironment of an organ while avoiding the biological and ethical complications associated with animal testing. Intestinal organoids are valuable tools for studying microbial-epithelial interactions[75–77] and may provide a key insight into the evaluation of new drugs by significantly increasing the efficiency and accuracy of in vitro validation and testing[78]. In our study, we confirmed the invasive properties of *E. coli* strain KV203, which was able to penetrate the organoid lumen. Importantly, the significant reduction of the bacterial load highlights the potential of RGD-Pac525 to target bacteria that have penetrated deep into epithelial layers, which a critical requirement for addressing chronic infections such as Crohn's disease-associated adherent-invasive *E. coli* (AIEC)[8]. Previous studies using intestinal organoids to evaluate antimicrobial agents against *E. coli* AIEC strains demonstrated limited success in reducing bacterial invasion without negatively affecting epithelial integrity[76]. In contrast, our results demonstrate that RGD-Pac525 effectively reduces intracellular bacterial burdens while maintaining organoid morphology. This offers a promising strategy for clinical applications in managing inflammatory diseases associated with intracellular bacterial infections.

The CAM model, utilized as a low-cost and ethical alternative to mammalian models, provided great insights into the infection dynamics and therapeutic potential of RGD-Pac525. We observed a marked reduction in the bacterial load in the liver and the intestinal tissues, indicating that the peptide was capable of systemic distribution and overcoming tissue barriers.

Similar studies have shown that CAM models effectively predict the systemic dissemination of intracellular pathogens[79] and assess the ability of therapeutic agents to mitigate this spread[80]. Previous studies have shown that chickens hatched from the eggs experimentally infected with *E. coli* exhibited reduced weight gain, and delayed yolk absorption[81] that corroborates our results. Studies such as those by Li et al. (2022) have demonstrated similar results using RGD-modified liposomal delivery systems, which achieved high efficacy in reducing bacterial counts across multiple organs in murine models and supported the therapeutic application of RGD-based delivery strategies[82]. The ability of RGD-Pac525 to penetrate intracellular spaces, cross tissue barriers, and remain effective in diverse biological environments highlights its potential for systemic administration. This is particularly relevant for treating conditions involving systemic bacterial dissemination, such as sepsis or invasive gastrointestinal infections where intracellular bacterial reservoirs pose a major challenge[83].

Our findings further revealed that untreated infections with *E. coli* KV203 led to substantial angiogenesis in the CAM, a response driven by bacterial lipopolysaccharides[84]. While our data can not conclusively differentiate direct anti-angiogenic effects of the peptide from indirect effects via bacterial reduction, the observed changes in angiogenesis were consistent with bacterial load reduction. Nevertheless, further experiments will be required to delineate these effects. Treatment with RGD-Pac525 significantly inhibited this angiogenic response and highlighted the peptide dual therapeutic role in managing bacterial infections and associated inflammatory responses. This observation aligns with previous studies showing that reducing infection induced angiogenesis can support tissue recovery and prevent further pathogen dissemination[85].

The combined use of organoids and CAM models in our study represents a robust animal-free approach addressing ethical considerations and the need for high-throughput preclinical testing. These models enable the evaluation of therapeutic candidates under conditions that closely mimic human physiology, thereby accelerating drug development while ensuring clinical relevance[75,86].

This study provides a proof of concept for the use of RGD-modified antimicrobial peptides in targeting intracellular bacterial infections. By employing organoid and CAM models, we demonstrated the efficacy of RGD-Pac525 in reducing bacterial load, managing infection-induced angiogenesis, and overcoming tissue barriers. Future research should focus on validating these findings in mammalian models, optimizing systemic delivery strategies, and assessing the efficacy of RGD-Pac525 against other IC pathogens. The promising effect of this peptide could fill gaps in current treatment options for intracellular as well as systemic bacterial infections.

## Conclusions

In conclusion, our study highlights the potential of the RGD-Pac525 peptide as an antimicrobial agent for treatment of intracellular bacterial infections, such as those caused by adherent-invasive pathotype *E. coli* KV203. The peptide effectively inhibited planktonic *E. coli*, showed no cytotoxicity at relevant concentrations, penetrated eukaryotic cell membranes, tissue barriers and exhibited antibacterial activity against intracellular bacteria in vitro. By utilizing innovative models such as chicken intestinal organoids and the CAM assay, this study provides insights into the peptide antimicrobial activity. These findings underscore the RGD-Pac525 unique ability to target and eliminate intracellular pathogens, indicating its potential for future clinical applications.

## Data availability

Data generated in this study are available from the corresponding author upon reasonable request. The Supplementary Material for this article is provided online.

Received: 25 February 2025; Accepted: 29 May 2025
Published online: 06 June 2025

## References

1. Kaufmann, S. H. E. Intracellular pathogens: living in an extreme environment. *Immunol. Rev.* **240**, 5–10 (2011).
2. Thakur, A., Mikkelsen, H. & Jungersen, G. Intracellular pathogens: Host immunity and microbial persistence strategies. *J. Immunol. Res.* **2019**, 1–24 (2019).
3. Anderson, G., Dodson, K., Hooton, T. & Hultgren, S. Intracellular bacterial communities of uropathogenic in urinary tract pathogenesis. *Trends Microbiol.* **12**, 424–430 (2004).
4. Conover, M. S. et al. Metabolic requirements of *Escherichia coli* in intracellular bacterial communities during urinary tract infection pathogenesis. *mBio* **7**, e00104–e00116 (2016).
5. Kaper, J. B., Nataro, J. P. & Mobley, H. L. T. Pathogenic *Escherichia coli*. *Nat. Rev. Microbiol.* **2**, 123–140 (2004).
6. Conte, M. P. et al. Adherent-invasive *Escherichia coli* (AIEC) in pediatric crohn's disease patients: phenotypic and genetic pathogenic features. *BMC Res. Notes*. **7**, 748 (2014).
7. Darfeuille-Michaud, A. et al. Presence of adherent *Escherichia coli* strains in ileal mucosa of patients with crohn's disease. *Gastroenterology* **115**, 1405–1413 (1998).
8. Darfeuille-Michaud, A. et al. High prevalence of adherent-invasive *Escherichia coli* associated with ileal mucosa in Crohn's disease. *Gastroenterology*. **127**, 412–421 (2004).
9. Darfeuille-Michaud, A. Adherent-invasive *Escherichia coli*: a putative new *E. coli* pathotype associated with crohn's disease. *Int. J. Med. Microbiol.* **292**, 185–193 (2002).
10. Buccini, D. F., Cardoso, M. H. & Franco, O. L. Antimicrobial peptides and Cell-Penetrating peptides for treating intracellular bacterial infections. *Front. Cell. Infect. Microbiol.* **10**, 612931 (2021).
11. Van Bambeke, F., Barcia-Macay, M., Lemaire, S. & Tulkens, P. M. Cellular pharmacodynamics and pharmacokinetics of antibiotics: current views and perspectives. *Curr. Opin. Drug Discov. Dev*. **9**, 218–230 (2006).
12. Dalhoff, A., Schubert, S. & Ullmann, U. Effect of pH on the in vitro activity of and propensity for emergence of resistance to fluoroquinolones, macrolides, and a ketolide. *Infection* **33**, 36–43 (2005).
13. Morales, L. D., Av-Gay, Y. & Murphy, M. E. P. Acidic pH modulates *Burkholderia cenocepacia* antimicrobial susceptibility in the cystic fibrosis nutritional environment. *Microbiol. Spectr.* **11**, e02731–e02723 (2023).
14. Nussbaumer-Pröll, A. K. et al. Low pH reduces the activity of ceftolozane/tazobactam in human urine, but confirms current breakpoints for urinary tract infections. *J. Antimicrob. Chemother.* **75**, 593–599 (2020).
15. Nussbaumer-Pröll, A. K., Eberl, S., Schober, C. & Zeitlinger, M. Impact of pH on the activity of novel cephalosporin Cefiderocol in human urine. *J. Antimicrob. Chemother.* **79**, 166–171 (2024).
16. Smith, C. B., Evavold, C. & Kersh, G. J. The effect of pH on antibiotic efficacy against Coxiella burnetii in axenic media. *Sci. Rep.* **9**, 18132 (2019).
17. Carryn, S. et al. Intracellular pharmacodynamics of antibiotics. *Infect. Dis. Clin. N. Am.* **17**, 615–634 (2003).
18. Lewies, A., Du Plessis, L. H. & Wentzel, J. F. Antimicrobial peptides: the achilles' heel of antibiotic resistance? *Probiotics Antimicrob. Proteins*. **11**, 370–381 (2019).
19. Magana, M. et al. The value of antimicrobial peptides in the age of resistance. *Lancet Infect. Dis.* **20**, e216–e230 (2020).
20. Moravej, H. et al. Antimicrobial peptides: features, action, and their resistance mechanisms in Bacteria. *Microb. Drug Resist.* **24**, 747–767 (2018).
21. Rima, M. et al. Antimicrobial peptides: A potent alternative to antibiotics. *Antibiotics*. **10**, 1095 (2021).
22. Steinstraesser, L., Kraneburg, U., Jacobsen, F. & Al-Benna Host defense peptides and their antimicrobial-immunomodulatory duality. *Immunobiology*. **216**, 322–333 (2011).
23. Mba, I. E. & Nweze, E. I. Antimicrobial peptides therapy: an emerging alternative for treating Drug-Resistant Bacteria. *Yale J. Biol. Med.* **95**, 445–463 (2022).
24. Mookherjee, N. & Hancock, R. E. W. Cationic host defence peptides: innate immune regulatory peptides as a novel approach for treating infections. *Cell. Mol. Life Sci.* **64**, 922–933 (2007).
25. Cudic, M. & Otvos, L. Jr. Intracellular targets of antibacterial peptides. *Curr. Drug Targets*. **3**, 101–106 (2002).
26. Ludwig, B. S., Kessler, H., Kossatz, S. & Reuning, U. RGD-Binding integrins revisited: how recently discovered functions and novel synthetic ligands (Re-)Shape an Ever-Evolving field. *Cancers*. **13**, 1711 (2021).
27. Wang, F. et al. The functions and applications of RGD in tumor therapy and tissue engineering. *Int. J. Mol. Sci.* **14**, 13447–13462 (2013).
28. Erdem Büyükkiraz, M. & Kesmen, Z. Antimicrobial peptides (AMPs): A promising class of antimicrobial compounds. *J. Appl. Microbiol.* **132**, 1573–1596 (2022).
29. Ahn, M. J. et al. Enhancement of antibacterial activity of short Tryptophan-rich antimicrobial peptide Pac-525 by replacing trp with His(chx). *Bull. Korean Chem. Soc.* **35**, 2818–2824 (2014).
30. Lau, Q. Y. et al. A Head-to-Head comparison of the antimicrobial activities of 30 Ultra-Short antimicrobial peptides against Staphylococcus aureus, Pseudomonas aeruginosa and Candida albicans. *Int. J. Pept. Res. Ther.* **21**, 21–28 (2015).
31. Qi, X. et al. Novel short antibacterial and antifungal peptides with low cytotoxicity: efficacy and action mechanisms. *Biochem. Biophys. Res. Commun.* **398**, 594–600 (2010).
32. Wei, S. Y. et al. Solution structure of a novel tryptophan-rich peptide with bidirectional antimicrobial activity. *J. Bacteriol.* **188**, 328–334 (2006).
33. Cuperus, T., Van Dijk, A., Matthijs, M. G. R., Veldhuizen, E. J. A. & Haagsman, H. P. Protective effect of in Ovo treatment with the chicken Cathelicidin analog D-CATH-2 against avian pathogenic E. coli. *Sci. Rep.* **6**, 26622 (2016).

34. Nguyen, T. T. T. et al. Avian antimicrobial peptides: in vitro and in Ovo characterization and protection from early chick mortality caused by yolk sac infection. *Sci. Rep.* **11**, 2132 (2021).
35. Verma, S., Senger, S., Cherayil, B. J. & Faherty, C. S. Spheres of influence: insights into Salmonella pathogenesis from intestinal organoids. *Microorganisms*. **8**, 504 (2020).
36. Zhang, Y. & Sun, J. Study Bacteria–Host interactions using intestinal organoids. In *Organoids*, vol 1576 (ed Turksen, K.) 249–254 (Springer New York, 2016).
37. Divya, M. et al. Biopolymer gelatin-coated zinc oxide nanoparticles showed high antibacterial, antibiofilm and anti-angiogenic activity. *J. Photochem. Photobiol. B*. **178**, 211–218 (2018).
38. Mitchell, J. et al. Chicken intestinal organoids: a novel method to measure the mode of action of feed additives. *Front. Immunol.* **15**, 1368545 (2024).
39. Chen, K. et al. Requirement of CRAMP for mouse macrophages to eliminate phagocytosed *E. coli* through an autophagy pathway. *J. Cell. Sci.* **134**, jcs252148 (2021).
40. Bosák, J. et al. Escherichia coli from biopsies differ in virulence genes between patients with colorectal neoplasia and healthy controls. *Front. Microbiol.* **14**, 1141619 (2023).
41. ISO. ISO 10993-5:2009 - Biological Evaluation of Medical Devices—Part 5: Tests for in Vitro Cytotoxicity. vol. ISO 10993-5:2009 34 (2009).
42. Elsinghorst, E. A. Measurement of invasion by gentamicin resistance. In *Methods in Enzymology*, vol. 236, 405–420 (Elsevier, 1994).
43. Bio-Rad Laboratories. Electroporation of *E. coli* using the gene pulser X-Cell electroporation system (2008).
44. Li, J. et al. Culture and characterization of chicken small intestinal crypts. *Poult. Sci.* **97**, 1536–1543 (2018).
45. Merlos Rodrigo, M. A. et al. Extending the applicability of in Ovo and ex Ovo chicken Chorioallantoic membrane assays to study cytostatic activity in neuroblastoma cells. *Front. Oncol.* **11**, 707366 (2021).
46. He, Y. et al. An antimicrobial Peptide-Loaded gelatin/chitosan nanofibrous membrane fabricated by sequential Layer-by-Layer electrospinning and electrospraying techniques. *Nanomaterials*. **8**, 327 (2018).
47. He, Y. et al. Development of an antimicrobial peptide-loaded mineralized collagen bone scaffold for infective bone defect repair. *Regen. Biomater.* **7**, 515–525 (2020).
48. He, Y. et al. A novel antibacterial titanium modification with a sustained release of Pac-525. *Nanomaterials*. **11**, 3306 (2021).
49. He, Y. et al. Composite mineralized collagen/polycaprolactone Scaffold-Loaded microsphere system with dual osteogenesis and antibacterial functions. *Polymers*. **16**, 2394 (2024).
50. Li, J. et al. High in vitro antibacterial activity of Pac-525 against *Porphyromonas gingivalis* biofilms cultured on titanium. *BioMed Res. Int.* **2015**, 1–8 (2015).
51. Zhang, Z. et al. Construction and characterizations of antibacterial surfaces based on Self-Assembled monolayer of antimicrobial peptides (Pac-525) derivatives on gold. *Coatings*. **11**, 1014 (2021).
52. Temming, K., Schiffelers, R. M., Molema, G. & Kok, R. J. RGD-based strategies for selective delivery of therapeutics and imaging agents to the tumour vasculature. *Drug Resist. Updat.* **8**, 381–402 (2005).
53. Abd El-Azeem, S. H., Khalil, A. A., Ibrahim, M. A. M. & Gamal, A. Y. The use of integrin binding domain loaded hydrogel (RGD) with minimally invasive surgical technique in treatment of periodontal intrabony defect: a randomized clinical and biochemical study. *J. Appl. Oral Sci.* **31**, e20230263 (2023).
54. Colin, M. et al. Liposomes enhance delivery and expression of an RGD-oligolysine gene transfer vector in human tracheal cells. *Gene Ther.* **5**, 1488–1498 (1998).
55. Cossu, J., Thoreau, F. & Boturyn, D. Multimeric RGD-based strategies for selective drug delivery to tumor tissues. *Pharmaceutics*. **15**, 525 (2023).
56. He, M. et al. Spatiotemporally controllable diphtheria toxin expression using a light-switchable transgene system combining multifunctional nanoparticle delivery system for targeted melanoma therapy. *J. Controlled Release*. **319**, 1–14 (2020).
57. Chen, C. W., Lu, Yeh, S. & Chiang Novel RGD-lipid conjugate-modified liposomes for enhancing SiRNA delivery in human retinal pigment epithelial cells. *Int. J. Nanomed.* **2567** https://doi.org/10.2147/IJN.S24447 (2011).
58. Jain, S. et al. RGD-anchored magnetic liposomes for monocytes/neutrophils-mediated brain targeting. *Int. J. Pharm.* **261**, 43–55 (2003).
59. Javid, H. et al. RGD peptide in cancer targeting: benefits, challenges, solutions, and possible integrin–RGD interactions. *Cancer Med.* **13**, e6800 (2024).
60. Shen, Z. et al. Small-sized gadolinium oxide based nanoparticles for high-efficiency theranostics of orthotopic glioblastoma. *Biomaterials*. **235**, 119783 (2020).
61. Wang, D. B. et al. Molecular magnetic resonance imaging of activated hepatic stellate cells with ultrasmall superparamagnetic iron oxide targeting integrin αvβ3 for staging liver fibrosis in rat model. *Int. J. Nanomed.* **1097** https://doi.org/10.2147/IJN.S101366 (2016).
62. Zhan, C. et al. Cyclic RGD conjugated poly(ethylene glycol)-co-poly(lactic acid) micelle enhances Paclitaxel anti-glioblastoma effect. *J. Controlled Release*. **143**, 136–142 (2010).
63. Manjusha, V., Reshma, L. R. & Anirudhan, T. S. Mesoporous silica gated mixed micelle for the targeted co-delivery of doxorubicin and Paclitaxel. *J. Drug Deliv. Sci. Technol.* **79**, 104032 (2023).
64. Raut, S. Y. et al. Engineered nano-carrier systems for the oral targeted delivery of follicle stimulating hormone: development, characterization, and, assessment of in vitro and in vivo performance and targetability. *Int. J. Pharm.* **637**, 122868 (2023).
65. Thakur, R., Suri, C. R., Kaur, I. P. & Rishi, P. Peptides as diagnostic, therapeutic, and theranostic tools: progress and future challenges. *Crit. Rev. Ther. Drug Carr. Syst.* **40**, 49–100 (2023).
66. Xu, Z. et al. RGD peptide modified RBC membrane functionalized biomimetic nanoparticles for thrombolytic therapy. *J. Mater. Sci. Mater. Med.* **34**, 18 (2023).
67. Kemker, I., Feiner, R. C., Müller, K. M. & Sewald, N. Size-dependent cellular uptake of RGD peptides. *ChemBioChem*. **21**, 496–499 (2020).
68. Diaferia, C., Rosa, E., Accardo, A. & Morelli, G. Peptide-based hydrogels as delivery systems for doxorubicin. *J. Pept. Sci.* **28**, e3301 (2022).
69. He, T. et al. Dual-stimuli-responsive nanotheranostics for dual-targeting photothermal-enhanced chemotherapy of tumor. *ACS Appl. Mater. Interfaces*. **13**, 22204–22212 (2021).
70. Juan, H. F. et al. Proteomics analysis of a novel compound: Cyclic RGD in breast carcinoma cell line MCF-7. *Proteomics*. **6**, 2991–3000 (2006).
71. Duarte-Mata, D. I. & Salinas-Carmona, M. C. Antimicrobial peptides´ immune modulation role in intracellular bacterial infection. *Front. Immunol.* **14**, 1119574 (2023).
72. Fang, Y. & Eglen, R. M. Three-dimensional cell cultures in drug discovery and development. *SLAS Discov.* **22**, 456–472 (2017).
73. Yan, J., Monlong, J., Cougoule, C., Lacroix-Lamandé, S. & Wiedemann, A. Mapping the scientific output of organoids for animal and human modeling infectious diseases: a bibliometric assessment. *Vet. Res.* **55**, 81 (2024).
74. Yao, Q. et al. Organoids: development and applications in disease models, drug discovery, precision medicine, and regenerative medicine. *MedComm*. **5**, e735 (2024).
75. Bozzetti, V. & Senger, S. Organoid technologies for the study of intestinal microbiota–host interactions. *Trends Mol. Med.* **28**, 290–303 (2022).

76. Forbester, J. L. et al. Interaction of Salmonella enterica serovar typhimurium with intestinal organoids derived from human induced pluripotent stem cells. *Infect. Immun.* **83**, 2926–2934 (2015).
77. Nickerson, K. P. et al. A versatile human intestinal organoid-derived epithelial monolayer model for the study of enteric pathogens. *Microbiol. Spectr.* **9**, e00003–21 (2021).
78. Schafer, S. T. et al. An in vivo neuroimmune organoid model to study human microglia phenotypes. *Cell.* **186**, 2111–2126e20 (2023).
79. Alnassan, A. A. et al. Embryonated chicken eggs as an alternative model for mixed Clostridium perfringens and Eimeria Tenella infection in chickens. *Parasitol. Res.* **112**, 2299–2306 (2013).
80. Ribeiro, L. N. M., Schlemper, A. E., da Silva, M. V. & Fonseca, B. B. Chicken embryo: a useful animal model for drug testing? *Eur. Rev. Med. Pharmacol. Sci.* **26**, 4828–4839 (2022).
81. Rezaee, M. S., Liebhart, D., Hess, C., Hess, M. & Paudel, S. Bacterial infection in chicken embryos and consequences of yolk sac constitution for embryo survival. *Vet. Pathol.* **58**, 71–79 (2021).
82. Li, G. et al. cRGD enables rapid phagocytosis of liposomal Vancomycin for intracellular bacterial clearance. *J. Controlled Release.* **344**, 202–213 (2022).
83. Kember, M., Grandy, S., Raudonis, R. & Cheng, Z. Non-Canonical host intracellular niche links to new antimicrobial resistance mechanism. *Pathogens* **11**, 220 (2022).
84. Pollet, I. et al. Bacterial lipopolysaccharide directly induces angiogenesis through TRAF6-mediated activation of NF-κB and c-Jun N-terminal kinase. *Blood*. **102**, 1740–1742 (2003).
85. Safari, Z. et al. Promotion of angiogenesis by M13 phage and RGD peptide in vitro and in vivo. *Sci. Rep.* **9**, 11182 (2019).
86. Kühl, L. et al. Human lung Organoids—A novel experimental and precision medicine approach. *Cells.* **12**, 2067 (2023).


## Acknowledgements

This work was financially supported by AF-IGA2023-IP-014. K.H. was supported by the project National Institute of Virology and Bacteriology (Programme EXCELES, ID Project No. LX22NPO5103) Funded by the European Union—Next Generation EU. The authors would like to thank the research group of David Šmajs (Faculty of Medicine, Masaryk University, Brno) for providing the clinical isolate of *Escherichia coli* KV203.

## Author contributions

All authors contributed to researching the data, writing their respective sections of the manuscript, and reviewing and editing the article. M.C. designed the experiments, executed the experimental work (including peptide labeling, microbiological tests, cell culture, and infection experiments), and prepared and wrote the manuscript. M.A.M.R. performed organoid and CAM assay experiments. H.M. supervised cell culturing and microscopy visualization. V.M. designed the antimicrobial peptide and supervised the peptide labeling. K.H. edited and prepared the final draft of the manuscript. L.Z. contributed to the experimental design and participated in editing and preparing the final draft. K.C. was responsible for experimental design, plasmid transformation, and the supervision of experiments.

## Declarations

## Competing interests

The authors declare no competing interests.

## Additional information

**Supplementary Information** The online version contains supplementary material available at https://doi.org/10.1038/s41598-025-04901-9.

**Correspondence** and requests for materials should be addressed to K.C.

**Reprints and permissions information** is available at www.nature.com/reprints.

**Publisher's note** Springer Nature remains neutral with regard to jurisdictional claims in published maps and institutional affiliations.